A Markov Chain Model for Coarse Timescale Channel Variation in an 802.16e Wireless Network

Anand Seetharam[1], Jim Kurose[1], Dennis Goeckel[2], Gautam Bhanage[3],
[1]Department of Computer Science,University of Massachusetts, Amherst MA 01003, USA
[2]Department of Electrical and Computer Engineering University of Massachusetts, Amherst MA 01003, USA
[3]WINLAB, Rutgers University, North Brunswick, 08902, USA
{anand, kurose}@cs.umass.edu, goeckel@ecs.umass.edu, gautamb@winlab.rutgers.edu

***Abstract*—A wide range of wireless channel models have been developed to model variations in received signal strength. In contrast to prior work, which has focused primarily on channel modeling on a short, per- packet timescale (millisecond), we develop and validate a finite-state Markov chain model that captures variations due to shadowing, which occur at coarser time scales. The Markov chain is constructed by partitioning the entire range of shadowing into a finite number of intervals. We determine the Markov chain transition matrix in two ways: *(i)* via an abstract modeling approach in which shadowing effects are modeled as a log-normally distributed random variable affecting the received power, and the transition probabilities are derived as functions of the variance and autocorrelation function of shadowing; *(ii)* via an empirical approach, in which the transition matrix is calculated by directly measuring the changes in signal strengths collected in a 802.16e (WiMAX) network. We validate the abstract model by comparing its steady state and transient performance predictions with those computed using the empirically derived transition matrix and those observed in the actual traces themselves.**

I. Introduction

A large number of finite-state Markov chain models have been proposed to study the wireless channel quality and the received signal strength, beginning with the early Gilbert and Elliot two-state Markov channel [1], [2]. Variation in received signal strength over a wireless channel is caused by three main factors: multipath fading, path loss and shadowing. Among these three effects, fading is caused by constructive or destructive effects of multipath waves and changes in the order of milliseconds depending on the speed of the receiver and the frequency of transmission. Conversely, shadowing and path loss cause fluctuations in the signal level in the order of seconds and tens of seconds respectively. Path loss is the deterministic distance-dependent component of the received power. Superimposed on path loss is shadowing - a random process that captures variations in the received signal caused by changes in the environment (buildings, foliage and motion in the surroundings). Informally, shadowing is the variation in signal strength at the seconds' timescale that is independent of the distance between the transmitter and receiver.

We focus on shadowing in this paper and develop and validate a Markov chain to model the effects of shadowing on the received signal strength, that occur on the order of seconds. This shadowing model can be used in analyzing performance of wireless network protocols (e.g., for route adaptation, or for video transmission) that adapt their behavior in response to link-level changes at the timescale of seconds. We discuss applications of coarse-timescale channel modeling in detail in Section II. The underlying physical channel model assumes that the variation in received signal strength due to shadowing is a lognormally-distributed random variable with zero mean [3] and has an exponential autocorrelation function [4]. An exponential autocorrelation function in turn implies that shadowing follows a First Order Autoregressive AR(1) process[5]. The AR(1) process is a Markov process [5] because the current value of the process at time t depends only the value at $t-1$. These assumptions together enable the construction of a Markov chain model that captures the impact of shadowing on received power. We divide the entire range of shadowing into a finite number of intervals with each interval corresponding to a state in the Markov chain. We then determine the transition matrix of the Markov chain, investigating two methods for determining this transition matrix:

- *Model-based transition matrix.* In this method we derive mathematical expressions for the transition probabilities of the Markov chain using the properties of shadowing (log-normal distribution and exponential autocorrelation). This approach is parsimonious in nature as the transition probabilities depend only on the variance (σ^2) and the exponent (ρ) of the exponential autocorrelation function of shadowing. We refer to the transition matrix derived using this approach as the analytical one.
- *Empirical transition matrix.* The transition matrix can also be determined by conducting real world experiments, collecting received signal strength measurements, extracting the shadowing values and then determining the transitions from one state to the other. We refer to the transition matrix derived using this approach as the empirical one.

We also perform signal strength measurements in a WiMAX (802.16e) network and validate the assumptions of the Markov chain model using real world data. We use hypothesis testing and determine that the log-normal assumption of shadowing is a valid one. However our experiments show that the autocorrelation function does not follow an exponential distribution and hence the Markovian behavior described above fails to hold in practice.

We then determine the values of the analytical and empirical transition matrices using the measurements collected. Finally

978-1-4673-0775-8/12/$31.00 ©2012 IEEE

we compare the results (steady state occupancies and the transient behavior of the Markov chain) obtained by the two approaches with the observed shadowing-state distributions and find that they are quite close to one another even though the Markovian assumption is not corroborated by empirical measurements.

The rest of paper is organized as follows. In Section II, we discuss related work. We describe our Markov chain model in Section III and describe two approaches for deriving its transition matrix in Section IV. The assumptions of the model are validated in Section V while a comparison of the experimental and analytical results are presented in Section VI. We finally conclude the paper in SectionVII.

II. Related Work and Applications

There is a great deal of research on developing Markov chain models for wireless channels, with the earliest work in this area being the simple, two-state model proposed by Gilbert and Elliot [1], [2]. We discuss several of these previous works here, focusing on those that are most closely related to our own work and highlighting the new contributions in this present paper. In [6] a range of signal-to-noise ratio (SNR)values represents a state in the Markov chain. Based on this assumption the authors provide analytical expressions for the state transition probabilities and error probabilities in each state. In [7] the authors investigate the accuracy of a first-order Markov model for the success/failure of data blocks. A detailed survey of various channel models along with a description of their evolution over time is available in [8]. Our work differs from these existing Markov chain models for wireless channels in the sense that we concentrate on modeling channel variations at a much coarser time granularity, typically in the order of a few seconds and use shadowing to construct our model. We also validate our assumptions and results obtained from the model using data collected via real world experiments in a variety of different settings.

We next survey literature specifically focused on characterizing the properties of shadowing. A thorough description of the different random processes causing variation in the received signal strength over the wireless channel is available in [3], [9]. The log-normal nature of shadowing has been reported in [3], [10] and other prior work. [4] was the seminal paper describing the autocorrelation of shadowing as being exponentially distributed.

Recent research has proposed refined versions of the auto-correlation depending on the environment. In [10] the authors propose a new autocorrelation model for shadowing in urban environments based on data collected in a Chinese city. The correlation properties of shadowing for an indoor channel have been studied in [11], [12]. The authors in [11] observed that shadowing is very environment specific and that correlation can be found in well-separated links if their environment is similar. Oesteges et. al perform an empirical characterization of the received power over a wireless channel in [13] for the outdoor-to-outdoor and indoor-to-indoor environment. They introduce several new aspects specific to multi-user distributed channels and also suggest that shadowing be divided into two components: a static and a dynamic one. Thus, while previous research on shadowing has focused primarily on the underlying process and on studying and characterizing the different properties (distribution, autocorrelation, cross-correlation) of shadowing itself, our work in unique in that we construct a Markov chain model assuming the log-normal distribution and exponential autocorrelation of shadowing.

Before describing our Markov chain model in detail we first discuss several applications where coarse-timescale channel prediction is potentially valuable; this will help motivate the application of the results of this work. The first application is the scheduling of multiple video streams over a 3G/WiMAX network with the objective of minimizing the number of playout jitters. Let us assume a simple time slotted scheme in which a video stalls if there is not enough data to play out in a timeslot. Such a model would require channel estimation from one timeslot to the other. Further to facilitate a smooth viewing experience the timeslots should be in the order of seconds instead of milliseconds to avoid experiencing large number of small glitches.

Bulk transfer of data in energy constrained mobile sensor nodes would be facilitated by coarse timescale prediction as it would provide ample time to the nodes to boot up from sleep when the channel is good and then transmit their data. Disconnection prediction and topology management in mobile ad-hoc networks would also be aided by channel quality prediction at a coarse time granularity. Rate control on a block of data is gaining popularity and a successful implementation of a block based scheme would require a coarse timescale channel model to predict channel variations from one block to the next (a block can take 1-2 seconds to be transmitted) coupled with a fine grained tracking of signal strength fluctuations within a block.

III. A Shadowing-based channel model

In this section we describe the Markov chain model for shadowing and discuss its applicability in mobile wireless systems. Previous theoretical and practical studies indicate that the average received power varies logarithmically with the distance between the transmitter and receiver; this is the deterministic path loss component of the received power. Superimposed on the path loss is log-normally distributed random shadowing, which takes into account the fact that the received signal strength at the same transmitter-to-receiver separation can vary due to changes in the environmental surroundings.

Let d, α, d_0 be the transmitter-to-receiver separation, the path loss coefficient and the close-in reference distance respectively. The received power $P_r(d)$ in [dBm] considering log-normal shadowing [3] is given by

$$P_r(d)[dBm] = \bar{P}_r(d_0) + 10\alpha log\frac{d}{d_0} + X \qquad (1)$$

where $\bar{P}_r(d_0)$ is the average received power at the reference distance d_0, the second term reflects the logarithmic dependence of received power on distance, and X is the shadowing - a zero-mean Gaussian random variable with variance σ^2 in [dB]. Therefore, (1) demonstrates the effect of shadowing on received power.

Shadowing (in dB) [3] is assumed to be $N(0, \sigma^2)$ while both its spatial and temporal autocorrelation functions are assumed to be exponential [4], [10], [14]. Let X_i and X_{i+n} be the shadowing samples at time i and $i+n$ respectively. There are n samples between i and $i+n$ and let the time difference between two consecutive samples be δt. The temporal autocorrelation between X_i and X_{i+n} is given by,

$$\rho_n = \frac{E[X_i X_{i+n}]}{\sigma^2} = e^{-\frac{n\delta t}{\tau}} \quad (2)$$

If the autocorrelation between two successive samples is denoted by $\rho = e^{-\frac{\delta t}{\tau}}$, we have $\rho_n = \rho^n$. We denote ρ as the autocorrelation coefficient.

An exponential autocorrelation function implies that the random process is a first-order autoregressive AR(1) process [5]. Therefore the shadowing samples form an AR(1) process [14], and we can write the following equation

$$X_i = \rho X_{i-1} + (1-\rho)e_i \quad (3)$$

where e_i is white noise and is $\sim N(0, \sigma_e^2)$. Furthermore e_i and X_{i-1} are independent of each other. X_i being an AR(1) process also implies that shadowing is a Markovian process [5]. This is evident from (3) as well, since X_i depends only on X_{i-1}.

Our Markov chain model for shadowing is constructed as follows. The entire range of shadowing is partitioned into a finite number of intervals (N), where each state of the Markov chain corresponds to one such interval. Let us assume that the shadowing range is divided in the following way; $(A_0, A_1....A_N)$ where A_0 and A_N correspond to $-\infty$ and ∞ respectively, as shadowing is Gaussian distributed. Let Y_i denote that the X value is between A_{i-1} and A_i. Therefore, the set $\{Y_i\}$ denotes the states of the Markov chain. The goal is to derive the state transition matrix of the Markov chain, i.e., the transition probabilities P_{ij} from range Y_i to range Y_j, $\forall i, j \in N$. We describe approaches for numerically computing the transition matrix in Section IV.

In this section we constructed a Markov chain model that captures the effects of shadowing on the received power. We note that the overall variation in received power can only be captured by modeling both the variation in the distance and in shadowing, as evident in (1). However, if we assume that the distance remains constant during the time interval of interest, changes in the signal strength can be represented by modeling the effects of shadowing alone. The distance/average signal strength may well change more slowly, and can be updated at the sender based on feedback from the receiver at a coarser timescale. This may be a valid assumption for most applications, especially for those with lower mobility operating over ad-hoc and 3G/ cellular networks. We discuss this issue further in Section VII.

IV. Determining the Transition Matrix

In this section we describe the analytical and empirical approaches for determining the transition matrix of the Markov model for shadowing.

A. Analytical Approach

From the previous section, we know that shadowing (X) is normally distributed and that it is a Markov process (3). We now determine the state transition probabilities ($P'_{ij}s$,) and begin by stating the following lemma.

Lemma 1: Two consecutive shadowing samples are jointly Gaussian

Proof: From (3), e_i and X_{i-1} are independent and both are themselves Gaussian. Hence e_i and X_{i-1} are jointly Gaussian. From the Cramer-Wold Device it is known that X_i and X_{i-1} will be jointly Gaussian if any linear combination of them is Gaussian. Any linear combination of X_i and X_{i-1} can be represented as

$$Z = \alpha X_i + \beta X_{i-1} = (\alpha\rho + \beta)X_{i-1} + \alpha(1-\rho)e_i \quad (4)$$

e_i and X_{i-1} are jointly Gaussian which means that Z is Gaussian. Hence using the Cramer-Wold Device we have that X_i and X_{i-1} are jointly Gaussian. ■

To calculate the transition probability P_{ij}, we must determine the probability of transitioning from range Y_i to range Y_j at any time step k. X_k and X_{k-1} being jointly Gaussian implies that $X_{k+1}|X_k \sim N(\rho x_k, \sigma^2(1-\rho^2))$. Moreover we have that $X_k \sim N(0, \sigma^2)$. Therefore, we have

$$\begin{aligned} P_{ij} &= P(X_{k+1} \in Y_j | X_k \in Y_i) \\ &= \frac{P(\{X_{k+1} \in Y_j\} \cap \{X_k \in Y_i\})}{P(\{X_k \in Y_i\})} \\ &= \frac{\int_{Y_i}(\int_{Y_j} f_{X_{k+1}|X_k}(x_2|x_1)dx_2) f_{X_k}(x_1)dx_1}{\int_{Y_i} f_{X_k}(x_1)dx_1} \end{aligned} \quad (5)$$

As the distributions of $X_{k+1}|X_k$ and X_k are Gaussian, $\int_{Y_j} f_{X_{k+1}|X_k}(x_2|x_1)dx_2$ and $\int_{Y_i} f_{X_k}(x_1)dx_1$ can easily be calculated using error functions. The absolute value of P_{ij} can then be numerically calculated, as the integral in the numerator can be easily solved using a mathematical package like MATLAB, once the values of ρ and σ have been determined.

B. Empirical Approach

The transition matrix can also be determined by performing signal strength measurements at the receiver for experiments conducted over any desired network. The first task is to extract the shadowing values by eliminating the deterministic distance dependent path loss. We then determine the states of the Markov chain to which each of the shadowing values correspond to. Therefore, we have the sequence of states through which the Markov chain has progressed. The subsequent step is to determine the number of transitions from each state to the others by observing the sequence of states. For example, suppose there are 6 states in all and that the sequence of states is $\{.....2, 4, 6, 2, 4.....\}$. The subsequence $\{2, 4\}$ means that we increment the number of transitions from state 2 to state 4 by one. The next transitions are from states 4 to 6, 6 to 2 followed by another transition from 2 to 4. Once all the transitions have been considered, we use the relative values of the numbers of transitions from state i to state j for all states j to determine the empirical transition probabilities from state i to all states j, P_{ij}.

In this paper we determine the parameters (σ, ρ) needed for the analytically-determined transition matrix and the directly observed transition probabilities $P_{i,j}$ in the empirical transition matrix from experiments conducted over a WiMAX network. From the received power measurements we first extract the shadowing values. The variance and autocorrelation coefficient of the shadowing values are then determined, which are used to obtain the transition matrix analytically. The shadowing values are also used to obtain the empirical transition matrix by observing the transitions between successive shadowing samples.

V. Validating the Model

In the preceding sections we developed a Markov chain model for channel prediction based on changes in the received signal strength due to shadowing. Our goal in this section and the next is to conduct real world experiments and extract the shadowing samples to *(i)* corroborate the underlying model assumptions - that shadowing follows a normal distribution and that the autocorrelation of shadowing has an exponential distribution, *(ii)* determine the transition matrix of the Markov chain analytically and empirically, from the data collected, and *(iii)* compare the analytically and empirically obtained transition matrices, and the channel performance predictions made via the Markov chain models using these transition matrices to assess the ultimate usefulness of our model.

A. WiMAX experiments

We collected data under varying levels of user mobility (pedestrian and vehicular) for experiments carried out over a 802.16e (WiMAX) network. Channel quality measurements were taken by continuously transmitting data from a base station and receiving them on a laptop. The WiMAX measurements were carried out outdoors for pedestrian and vehicular mobility cases. Stationary outdoor measurements were also taken but changes in signal strength were found to be confined to a 4 dBm range. This implies that the channel essentially remains invariant and thus of little interest to us. Hence we do not explore this case any further here.

The WiMAX experiments were carried out at WINLAB in New Jersey, where the base station is mounted on the roof of a WINLAB building. The frequency of transmission for WiMAX is 2.59 GHz and its range is approximately 500m. We note that the diversity of our measurements would have increased if the experiments were conducted in different physical locations, as shadowing is dependent on the environment. But with only one WiMAX base station available, all measurements were taken within the campus. We look forward to future studies that will build on this initial modeling and measurement work.

The distance variation from the outdoor base station was captured using a GPS device attached to the laptop. The GPS device provided latitude and longitude information, which was then converted to 2D-Cartesian coordinates. The height of the base station from the ground was also measured and the transmitter-to-receiver distances calculated from this information.

We obtain signal strength quality one second apart from each another. To eliminate any fast fading effects, we consider the average signal strength at the beginning of each second. The average signal strength at the beginning of each second is obtained by averaging approximately 5 received power samples during a 50 ms period centered around the integer-values time (second) value. The shadowing samples were extracted by observing the deviation of the received power samples from the log distance relation. In all, three vehicular and two pedestrian traces were collected, each having a duration of approximately 8 minutes.

1) Normality Testing of Shadow Samples: We use the *Kolmogorov-Smirnov* goodness of fit test to determine the normality of shadowing for the traces collected. Let σ^2_{sam} denote the variance of the collected samples for any trace considered. The null hypothesis is the following: The samples are drawn from a normal distribution having mean 0 and variance σ^2_{sam}. Our tests failed to reject the null hypothesis at any acceptable level of significance for both the vehicular and pedestrian traces. The smoothed probability distribution obtained for one of the vehicular traces using the kernel density estimation method and the corresponding normal distribution are shown in Figure 1. The standard deviation for this trace is 4.4 dB.

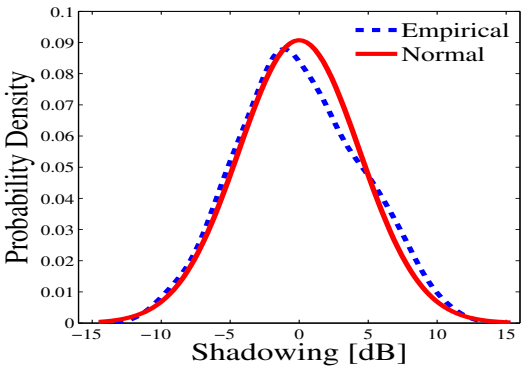

Fig. 1. WiMAX: Shadow Samples follow a Normal Distribution

2) Testing for Exponential Autocorrelation: The temporal autocorrelation function of shadowing for the three different vehicular traces along with the mean of these three traces is shown in Figure 2. We observe that the autocorrelation function does *not* follow an exponential distribution when the traces are considered individually. The data for pedestrian mobility in Figure 3 similarly shows that the autocorrelation function for these traces does not have an exponential distribution. Moreover, while we observed that the average autocorrelation was roughly exponentially distributed for the case of vehicular mobility, this is not the case for pedestrian mobility.

B. WiFi Experiments

The results reported in this paper are mostly for an outdoor WiMAX network. However our model is not restricted to that particular scenario and can be applied, for example, to an indoor setting like 802.11g (WiFi). We validate the log-normal distribution and exponential autocorrelation of shadowing for

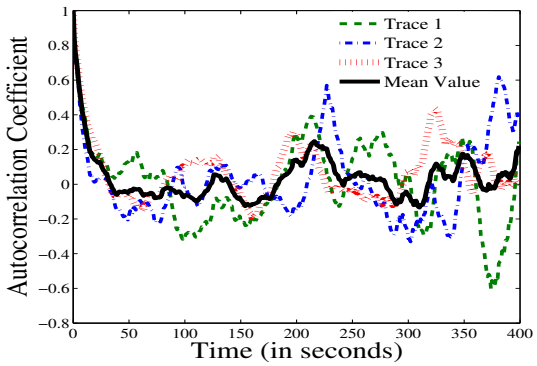

Fig. 2. WiMAX: Autocorrelation of Shadow Samples (Vehicular Mobility)

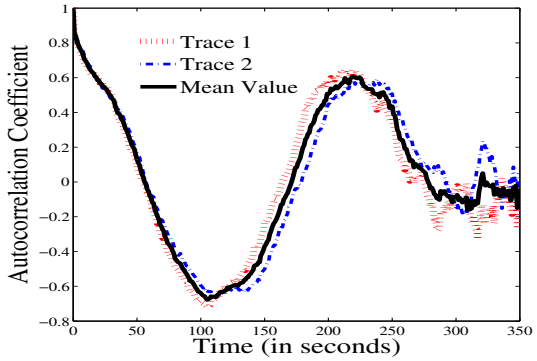

Fig. 3. WiMAX: Autocorrelation of Shadow Samples (Pedestrian Mobility)

the WiFi case and report the results here. However due to difficulty in collecting a sufficient amount of data, we were not able to compute the empirical transition matrix and compare the steady state and transient distributions of the Markov chain for the WiFi experiments.

The WiFi experimental setup consisted of 2 laptops, each with 802.11g wireless cards. The frequency of transmission was 2.412 GHz. The transmitter was kept inside a room while measurements were taken by moving down the hallway with the receiver. As GPS data cannot be collected indoors, the transmitter-to-receiver distances were calculated manually in this indoor setting. The transmitter was configured to send data packets continuously and received signal strength measurements were taken at the receiver at distances 1 feet apart. In all, a total of 140 data points were collected over a distance of 140 feet. To eliminate the effects of fading, the average received power at each location was calculated by considering a total of 5000 packets. We gathered data in this manner (e.g., rather than walking continuously) because we found that it was very difficult to assess the speed of walking and significant errors could be introduced if the relationship between received power and distance was incorrect. Due to the limited transmitter range, it was not possible to collect a large amount of data indoors.

Shadowing can depend strongly on the environment and so we collected data in three different settings using the setup described above. Two of the measurements were made in the Computer Science building at UMASS (a new building with more metal in it), while the other measurement was conducted in the Engineering building (a relatively older building with more concrete in it). The next task was to determine the distribution and autocorrelation function of shadowing in these settings.

We again observe that shadowing follows a normal distribution and our tests failed to reject the null hypothesis at reasonable levels of significance. The autocorrelation of the individual traces however, was not found to have an exponential distribution, as in the case of our WiMAX measurements. However, the average autocorrelation once again was found to be approximately exponential. This fact is evident in Figure 4.

Our WiMAX and WiFi experiments indicate the following. Our shadowing measurements indeed follow a normal distribution in both outdoor and indoor environments, for both pedestrian and vehicular mobility. The autocorrelation, however, can be expected to be exponential only on average and not for the individual traces. This also implies that shadowing does not satisfy one of the requirements needed for a Markovian model. In the following section we will see, however, that in spite of the fact that shadowing does not satisfy both properties needed to make it a Markov process, a Markov chain model based on Markovian assumptions can still be used to accurately predict performance measures of interest.

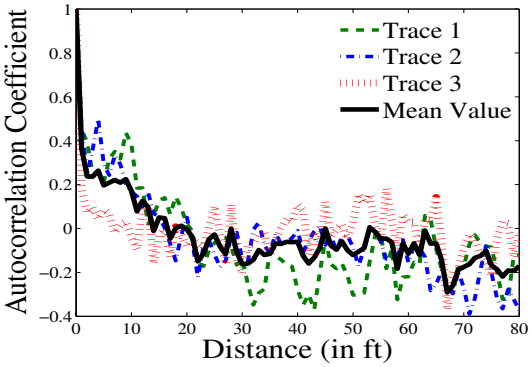

Fig. 4. WiFi: Autocorrelation of Shadow Samples

VI. Results

In this section we construct the Markov chain by dividing shadowing into the following intervals $\{-\infty, -\sigma_{sam}, -\frac{\sigma_{sam}}{2}, 0, \frac{\sigma_{sam}}{2}, \sigma_{sam}, \infty\}$. The size of the intervals is chosen in this manner so that there are sufficient data points in each interval. As shadowing follows a normal distribution the probability of receiving shadow samples becomes very small as we move away from the mean and so we consider the interval beyond $mod(\sigma_{sam})$ as an open interval.

We then determine the transition matrix analytically and empirically for the different vehicular and pedestrian traces using the approaches outlined in Section IV. We compute the standard deviation and autocorrelation coefficient needed to determine the analytic transition matrix. Table I lists these values for the vehicular and pedestrian traces. As expected, the

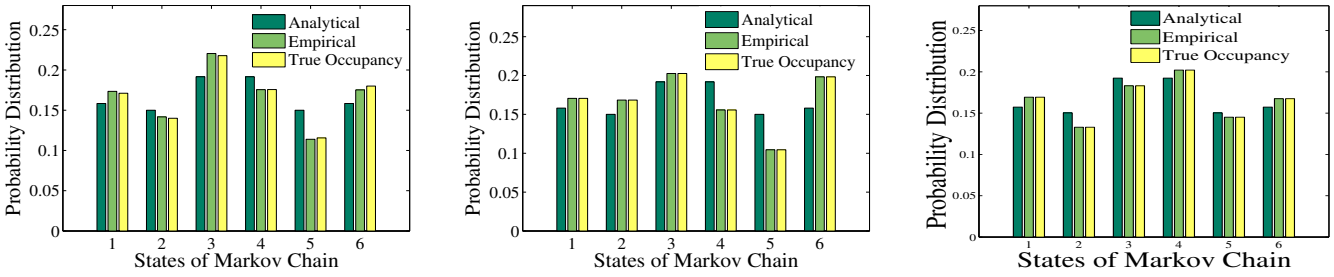

(a) Trace 1 (b) Trace 2 (c) Trace 3

Fig. 5. Comparison of analytical and empirical steady state occupancies of the Markov chain with the observed occupancy: Vehicular Mobility

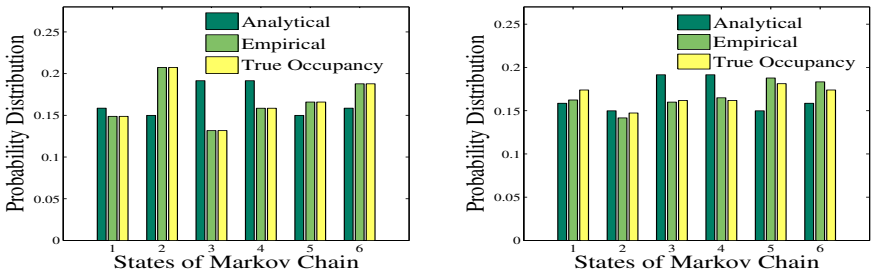

(a) Trace 1 (b) Trace 2

Fig. 6. Comparison of analytical and empirical steady state occupancies of the Markov chain with the observed occupancy: Pedestrian Mobility

		Standard Deviation	Autocorrelation Coefficient
Vehicular	Trace 1	4.4	0.84
	Trace2	4.3	0.83
	Trace 3	4.6	0.86
Pedestrian	Trace 1	3.6	0.84
	Trace 2	3.6	0.87

TABLE I
STANDARD DEVIATION AND AUTOCORRELATION COEFFICIENT

	State 1	State 2	State 3	State 4	State 5	State 6
State 1	0.6433	0.2334	0.0983	0.0211	0.0023	0.0001
State 2	0.2471	0.3290	0.2811	0.1169	0.0235	0.0024
State 3	0.0815	0.2202	0.3374	0.2519	0.0915	0.0175
State 4	0.0175	0.0915	0.2519	0.3374	0.2202	0.0815
State 5	0.0024	0.0235	0.1169	0.2811	0.3290	0.2471
State 6	0.0001	0.0023	0.0211	0.0983	0.2334	0.6433

TABLE II
VEHICULAR: ANALYTICAL TRANSITION MATRIX

	State 1	State 2	State 3	State 4	State 5	State 6
State 1	0.6883	0.2078	0.0909	0	0	0.0130
State 2	0.2381	0.3651	0.3016	0.0794	0	0.0159
State 3	0.0619	0.1649	0.4948	0.1856	0.0515	0.0412
State 4	0.0380	0.0633	0.2152	0.4304	0.1519	0.1013
State 5	0	0.0192	0.0577	0.2885	0.3846	0.2500
State 6	0	0.0244	0.0488	0.0854	0.1829	0.6585

TABLE III
VEHICULAR: EMPIRICAL TRANSITION MATRIX

values for the vehicular trace are close to one another while the same is true for the pedestrian traces. Tables II and III show the analytical and empirical transition matrix respectively for the vehicular trace whose distribution is characterized in Figure 1. Having determined the transition matrices, the ensuing step is to examine the closeness of the system state behavior (e.g., steady state and transient behavior), as calculated via one of the Markov chain models, and as observed empirically.

A. Steady State Behavior

In this subsection we obtain the steady state distributions using the analytical and empirical transition matrices. We then compare them with the empirically observed shadowing-state occupancies (True Occupancy). The True Occupancy is calculated by counting the number of shadowing samples in each interval and then normalizing them by the total number of samples. Figures 5 and 6 show the steady state behavior for the 3 vehicular and 2 pedestrian traces respectively. We observe that in terms of the steady state distribution, the parsimonious analytical approach and the empirical method match the true occupancies very closely. Figures 5 and 6 show good agreement in the model-predicted and observed steady state shadowing values, in spite of the lack of exponential autocorrelation evidenced in Figures 2 and 3.

B. Transient Behavior

Having studied and validated the steady state behavior in the previous subsection, we focus on the transient state analysis here. We begin by determining the empirically observed distribution of transitioning to the different shadowing states as a function of the number of time steps (starting from any state). For example, from the traces collected, we calculate the probability of transitioning to the other states after 2 time steps starting from say, state 3. We once again refer to this as the True Occupancy. The transition probability distribution as a function of the number of time steps is also obtained from the analytical and empirical transition matrices. As the number of

		Mean (2 step)	Variance (2 step)	Mean (5 step)	Variance (5 step)
Trace 1	Anal	3.19	1.99	3.35	2.64
	Emp	3.21	1.88	3.34	2.67
	True	3.08	1.57	3.2	2.28
Trace 2	Anal	3.19	1.99	3.35	2.63
	Emp	3.17	1.95	3.30	2.77
	True	3.29	1.89	3.5	2.88
Trace 2	Anal	3.17	1.8	3.3	2.54
	Emp	3.29	1.94	3.42	2.66
	True	3.16	1.19	3.47	2.47

TABLE IV
TRANSIENT STATE BEHAVIOR: VEHICULAR MOBILITY

		Mean (2 step)	Variance (2 step)	Mean (5 step)	Variance (5 step)
Trace 1	Anal	3.18	1.93	3.33	2.6
	Emp	2.86	2.0	3.1	2.75
	True	2.78	1.06	2.86	1.57
Trace 2	Anal	3.15	1.74	3.30	2.52
	Emp	3.12	1.79	3.33	2.78
	True	3.06	0.92	3.07	1.05

TABLE V
TRANSIENT STATE BEHAVIOR: PEDESTRIAN MOBILITY

time steps increase the transient behavior will approach steady state.

We study the transient behavior of the Markov chain by comparing the first and second moments (the mean and variance) of the distributions obtained by the various approaches. We assign numerical values 1 through 6 for the different states of the Markov Chain. The states of the Markov chain being abstract, the absolute values of the mean and variance do not have any physical interpretation. The goal of this analysis is to compare the moments obtained by the different methods to determine the closeness of the distributions. For sake of conciseness we represent the 2 and 5 time step transitions from state 3 in Tables IV and V for the vehicular and pedestrian traces respectively. From Table IV we observe that the mean and variance obtained by the analytical and empirical methods are close to true occupancies for the vehicular mobility scenario. For the pedestrian mobility scenario, the performance of the analytical and empirical methods is comparable to one another. But unlike the vehicular mobility case, their performance is not that close to the True Occupancy. We also studied the transition probability distribution from the other states graphically for the vehicular and pedestrian traces and similarly observed that performance of the empirical and analytical approaches were comparable but were sometimes not that close to the True Occupancy.

We also compare the different distributions in terms of the total variation [15]. The total variation between a probability distribution P and a probability distribution Q with n outcomes is given by,

$$Total\ \ Variation = \frac{1}{2}\sum_{i=1}^{n}|p_i - q_i| \qquad (6)$$

Tables VI and VII present the 2 and 5 time step total variation between the analytical and true occupancies as well as the empirical and true occupancies for the vehicular and pedestrian traces respectively. We observe from these tables that the total variation is small, which implies that the distributions are close to each other. Once again, we observe that the vehicular mobility results are better than the pedestrian mobility case. We would like to note here that the after about 25 steps, the probability distribution obtained by the analytical and empirical transition matrices from any state reaches very close (5%) to the steady state distribution for all the vehicular and pedestrian mobility cases.

	Anal-True (2 step)	Emp-True (2 step)	Anal-True (5 step)	Emp-True (5 step)
Trace1	0.15	0.10	0.06	0.08
Trace2	0.22	0.11	0.11	0.06
Trace3	0.13	0.14	0.07	0.05

TABLE VI
TOTAL VARIATION: VEHICULAR MOBILITY

	Anal-True (2 step)	Emp-True (2 step)	Anal-True (5 step)	Emp-True (5 step)
Trace1	0.21	0.20	0.20	0.16
Trace2	0.22	0.21	0.31	0.33

TABLE VII
TOTAL VARIATION: PEDESTRIAN MOBILITY

Our analysis of the steady state and transient behavior shows that the Markov chain model has good agreement between the model-predicted and true distributions, though the assumption of shadowing having an exponential autocorrelation function is violated.

VII. CONCLUSION

In this paper, we presented a channel prediction model based on shadowing. The total received signal strength is dependent both on distance and shadowing. If we assume that the distance remains unaltered during the time period of interest, we can just rely on shadowing to capture the variations in signal strength. However in situations where the above premise does not hold true one can combine the shadowing-based Markov chain model with a mobility one to model signal strength fluctuations. A complete and thorough survey of the different mobility models and their applicability in various scenarios can be found in [16]. Depending on the type of mobility, one can choose the appropriate model and then combine it with the shadowing based one to model the variations in the overall received power. We plan to pursue this as future work.

In conclusion, we can say that we developed and validated a finite-state Markov chain channel model to capture wireless channel variations due to shadowing. We obtain the Markov chain transition matrix in two ways: (i) via a parsimonious modeling approach in which shadowing effects are modeled as a log normally distributed random variable affecting the received power, and the transition probabilities are derived as functions of the variance and autocorrelation function of shadowing; (ii) via an empirical approach, in which the Markov chain transition matrix is calculated by directly measuring the changes in signal strengths collected in an 802.16e (WiMAX) network. The model validation showed that the assumption that the variation in received signal strength due to shadowing had a lognormally-distributed random variable was a good one, but

that the assumption of an exponential autocorrelation function was violated. Nonetheless, the Markov chain model showed good agreement between the model-predicted and observed values of shadowing for both the steady state and transient behavior.

VIII. Acknowledgement

This research was sponsored by the National Science Foundation under grants CNS-1018464 and CNS-1040781, and by the US Army Research laboratory and the UK Ministry of Defense and was accomplished under Agreement Number W911NF-06-3-0001. The views and conclusions contained in this document are those of the authors and should not be interpreted as representing the official policies, either expressed or implied, of the US Army Research Laboratory, the U.S. Government, the UK Ministry of Defense, or the UK Government. The US and UK Governments are authorized to reproduce and distribute reprints for Government purposes notwithstanding any copyright notation hereon.

References

[1] E. Gilbert, "Capacity of a burst-noise channel," *Bell Syst. Tech. Journal*, vol. 39, 1960.
[2] E. Elliot, "Estimates of error rates for codes on burst-noise channels," *Bell Syst. Tech. Journal*, vol. 42, 1963.
[3] T. Rappaport, *Wireless Communications: Principles and Practice*. Prentice Hall, 2002.
[4] M. Gudmundson, "Correlation model for shadow fading in mobile radio systems," *Electronic Letters*, vol. 27, no. 23, 1991.
[5] W. W. Wei, *Time Series Analysis: Univariate and Multivariate Methods*. Pearson Addison Wesley, 2006.
[6] H. S. Wang and N. Moayeri, "Finite-state markov channel- a useful model for radio communication channels," *IEEE Trans. On Vehicular Technology*, vol. 44, no. 1, 1995.
[7] M. Zorzi, R. Rao, and L. Milstein, "On the accuracy of a first-order markov model for data block transmission on fading channels," in *IEEE ICUPC*, 1995.
[8] P. Sadeghi, R. A. Kennedy, P. Rapajic, and R. Shams, "Finite-state markov modeling for fading channels- a survey of principles and applications," *IEEE Signal Processing Magazine*, vol. 25, no. 5, 2008.
[9] D. Tse and P. Vishwanath, *Fundamentals of Wireless Communication*. Cambridge University Press, 2005.
[10] Y. Zhang, J. Zhang, D. Dong, X. Nie, G. Liu, and P. Zhang, "A novel spatial autocorrelation model of shadow fading in urban macro environments," in *IEEE GLOBECOM*, 2008.
[11] N. M. Jalden, P. Zetterberg, B. Ottersten, A. Hong, and R. Thoma, "Correlation properties of large scale fading based on indoor measurements," in *IEEE PIMRC*, 2007.
[12] R. Sharma and J. Wallace, "Indoor shadowing correlation measurements for cognitive radio systems," in *IEEE APSURSI*, 2009.
[13] C. Oestges, N. Czink, B. Bandemer, and P. Castigoline, "Experimental characterization and modeling of outdoor-to-outdoor and indoor-to-indoor distributed channels," *IEEE Trans. On Vehicular Technology*, vol. 59, 2010.
[14] J. Wui, S. Affes, and P. Mermelstein, "Forward-link soft-handoff in cdma with multiple-antenna selection and fast joint power control," *IEEE Trans. on Wireless Comm.*, vol. 2, no. 3, 2003.
[15] D. A. Levin, "Coupling ams short course, university of oregon."
[16] N. Aschenbruck, E. Gerhards-Padilla, and P. Martini, "A survey on mobility models for performance analysis in tactical mobile networks," *Journal of Telecommunications and Information Technology*, 2008.